17th World Conference on Earthquake Engineering, 17WCEE
Sendai, Japan - September 13th to 18th 2020

DECISION-ORIENTED COLUMN SIMULATION CAPABILITIES FOR ENHANCING DISASTER RESILIENCE OF RC BUILDINGS

W. Ghannoum[(1)], A. Matamoros[(2)], S. Breña [(3)], A. Suselo[(4)], R. Ghorbani[(5)], S. Gendy[(6)], N. Zad[(7)], A. Al-Sammari[(8)]

[(1)] *Associate Professor, University of Texas at San Antonio, wassim.ghannoum@utsa.edu*
[(2)] *Professor, University of Texas at San Antonio, adolfo.matamoros@utsa.edu*
[(3)] *Professor, University of Massachusetts, Amherst, brena@umass.edu*
[(4)] *PhD Candidate, University of Texas at San Antonio, ariel.suselo@utsa.edu*
[(5)] *PhD Candidate, University of Texas at San Antonio, rasool.ghorbani@utsa.edu*
[(6)] *Former Post-Doctoral Research Scientist, University of Texas at San Antonio, samersabry2005@hotmail.com*
[(7)] *PhD Candidate, University of Texas at San Antonio, nader.zad@utsa.edu*
[(8)] *Post-doctoral Research Associate, University of Massachusetts, Amherst, aalsamma@engin.umass.edu*

Abstract

Improving the resilience of structures to earthquake demands requires improving the accuracy and transparency of damage assessments, as well as the implementation of new strategies for limiting damage during strong shaking. Unfortunately, current standardized and non-standardized methods for design, evaluation, and retrofit are stymied in reaching goals of improved seismic performance and recovery times by several challenges: the most outstanding of which being the lack of reliable decision-oriented simulation capabilities. The objective of the research work presented is to fill this critical gap by developing enhanced simulation capabilities for reinforced concrete columns subjected to severe earthquake demands. The project focuses on concrete columns because they represent the most critical threat to seismic safety and resilience. The proposed simulation element and associated tools go beyond the traditional force-deformation computational space and deliver critical engineering data that enables informed decisions for enhancing seismic resilience. The proposed tools can deliver metrics for damage type and extent, for residual capacities applicable to post-event recovery evaluations, and for retrofitted capacities in support of retrofit decisions. The metrics also provide critical data needed to the development of the next generation of performance-based seismic standards. The column simulation model is calibrated to all major failure modes in concrete columns, including flexural, splice, shear and axial failures. It is implemented in OpenSEES and has the ability to simulate coupled shear-flexure-axial behavior. The model is also capable of simulating the full cyclic behavior of retrofitted columns. While users can input manually any parameter of the model, in its calibrated format the model only requires the input of column material and geometric properties to fully calibrate its multi-axial behavior; thus facilitating use by the profession. To capture the effects of damage progression and residual strength, a new damage model is implemented that takes monotonic-pushover backbone relations derived from test data and nonlinear continuum finite element analyses and adjusts response due to cyclic damage effects. The model can explicitly simulate axial failure and the nonlinear axial degrading behavior, which can permit engineers to explore the full extent of structural redundancies and load redistributions. Such capabilities can therefore aid in refining retrofit strategies and greatly reduce rehabilitation costs. An associated web tools is designed to let users explore different column design and retrofit schemes by running any deformation history through the column model and observing changes in response and damage levels. The tool can also utilize the exported damage state of a column from a nonlinear analysis and run it through prescribed deformation histories to assess its residual capacities. An overview of key novel aspects of the computational element is presented.

Keywords: concrete columns; simulation; collapse; residual capacity; retrofit.

1. Introduction

The Christchurch earthquake of 2011 as well as other recent earthquakes have highlighted critical shortcomings that are limiting the seismic resilience of building infrastructure: 1) older non-ductile concrete buildings pose a severe threat to loss of life during strong earthquake shaking; 2) buildings meeting the latest seismic design standards can be expected to suffer damage extensive enough to require costly and time consuming repairs, or warrant demolition; and 3) the structural engineering community has close to non-existent post-earthquake residual capacity evaluation methodologies that are critical for disaster recovery.

Unfortunately, the tools that are currently available to structural engineers for evaluating building seismic performance and making informed retrofit, repair or enhanced-design decisions, have many gaps. These gaps have resulted in crude performance metrics, which do not lend themselves to streamlining decisions for enhancing the seismic resilience of new building designs, nor to optimizing retrofits often resulting in costly measures. For example, no methods are currently available that quantify reductions in the level of damage resulting from detailing changes in concrete members. Consequently, the life-cycle cost benefits of enhancement measures are currently difficult to evaluate, and require extensive interjection of engineering judgement, which in turn causes objectivity to be lost in the process. Moreover, the primary seismic evaluation and retrofit standards used in the U.S., ASCE/SEI 41-17 [1] and ACI 369.1-17 [2] that provide the most advanced standardized framework for addressing the seismic resilience of buildings, have been shown to produce overly conservative estimates of building seismic capacities, resulting in costly building retrofits that discourage interventions and render efforts to enhance community resilience to major earthquakes less tractable. Moreover, recent National Institute of Standards and Technology (NIST) studies [3] have uncovered severe inconsistencies between ASCE/SEI 41-17 and the primary design standard for modern concrete buildings, ACI 318-19 [4]. These inconsistencies have brought challenges to both standards, which further contributed to inaction towards increased disaster resilience.

Recognizing the limitations of current standards, several studies have attempted to fill some of the gaps and provide engineers with more powerful and refined tools for improving estimates of seismic performance. However, concrete columns subjected to large deformations under strong earthquake shaking can exhibit a number of strength degradation modes, mainly those induced by: shear forces, anchorage failure, flexural demands, loss of concrete confinement, and axial forces. Complicating matters further is the fact that numerous interactions occur between column actions (i.e., axial, bending and shear), and degradation mechanisms; for example, shear and confinement mechanisms often interact as they depend on the integrity of the core concrete. Few available column simulation models possess the required advanced capabilities, and when they do, it is only for a subset of degradation mechanisms. The state-of-the-art in column tools and their limitations were summarized in a 2013 NIST report [5]. The report highlights that the available models and tools for concrete columns are highly fragmented by strength degradation mechanisms and typically incomplete with respect to simulating the load-path dependent cyclic behavior (e.g., [6, 7, 8, 9]). None of the column models currently found in the literature offer direct damage estimation. Instead, they deliver force-deformation behaviors from which column damage states have to be inferred. Few models exist for simulating the response of retrofitted columns, none of which providing guidance on selecting the cyclic behavioral rules. Fiber-element models that incorporate constitutive rules of FRP-confined concrete and spliced steel are promising but lack generality [10]. Given the variety of retrofitting techniques used in columns with deficient details, existing models are not universal and have only been calibrated using limited sets of test results.

The objective of the research work presented is to fill current critical gaps by developing enhanced simulation capabilities for reinforced concrete columns subjected to severe earthquake demands. The project focuses on concrete columns because they represent the most critical threat to seismic safety and resilience. The proposed simulation element and associated tools go beyond the traditional force-deformation computational space and deliver critical engineering data that enables informed decisions for enhancing seismic resilience. The proposed tools can deliver metrics for damage type and extent, for residual capacities

applicable to post-event recovery evaluations, and for retrofitted capacities in support of retrofit decisions. The metrics also provide critical data needed to the development of the next generation of performance-based seismic standards. The column simulation model is calibrated to all major failure modes expected in concrete columns in buildings, including flexural, splice, shear and axial failures. It is implemented in OpenSEES [11] and has the ability to simulate coupled shear-flexure-axial behavior. The model is also capable of simulating the full cyclic behavior of retrofitted columns. While users can input manually any parameter of the model, in its calibrated format the model only requires the input of column material and geometric properties to fully calibrate its multi-axial behavior; thus facilitating use by the profession. To capture the effects of damage progression and residual strength, a new damage model is implemented that takes monotonic-pushover backbone relations derived from test data and nonlinear continuum finite element analyses and adjusts response due to cyclic damage effects. The model can explicitly simulate axial failure and the nonlinear axial degrading behavior, which can permit engineers to explore the full extent of structural redundancies and load redistributions. Such capabilities can therefore aid in refining retrofit strategies and greatly reduce rehabilitation costs. An associated web tools is designed to let users explore different column design and retrofit schemes by running any deformation history through the column model and observing changes in response and damage levels. The tool can also utilize the exported damage state of a column from a nonlinear analysis of a building and run it through prescribed deformation histories to assess its residual capacities. An overview of key novel aspects of the computational element is presented.

2. Proposed Computational Element

A lumped-plasticity computational framework was selected as the basis for the proposed model since such a framework is computationally efficient and allows a greater degree of control in calibrating the degrading and cyclic behaviors of concrete columns. When considering the task of assessing the seismic vulnerability of building structures using nonlinear dynamic procedures, current standards (e.g. [1, 12]) require subjecting a building model to numerous ground motions (11 or more). Moreover, when engineers investigate retrofit schemes to optimize rehabilitation measures, several more analyses need to be conducted. Due to the sheer number of nonlinear dynamics analyses that are requires in the process, continuum finite element modeling approaches are computationally prohibitive and were precluded from consideration in the project. Fiber-based models, in which the cross-section of the member is subdivided into longitudinal fibers and the behavior of each fiber is represented based on stress-strain relationship for concrete or steel bars, are more computationally efficient than continuum models and offer advantages in modeling axial-flexure interactions. However, these modeling techniques cannot account for the coupling of axial, flexural and shear behaviors. Furthermore, fiber-models are difficult to calibrate to achieve observed strength degradation and cyclic damage behaviors. A detailed explanation of these modeling techniques can be found in [13, 14].

Lumped-plasticity behavioral models can be broadly classified into two groups: (i) pre-defined models having parameters that remain static during analysis, and (ii) adaptive models that monitor varying quantities during analysis and adjust their parameters accordingly. In the first category of models, polygonal hysteresis (PH) rules that use two or three straight lines to simulate stiffness changes during cyclic loading are typically used. Reviews of such models are presented in several publications [e.g., 15, 16, 17, 18, 19, 20, 21]. These models usually require an extensive number of input parameters that lack physical interpretation to define the prominent characteristics of the cyclic properties of the responses. Moreover, current models do not represent the coupling behavior as each uniaxial model constructs the load-deformation response for each degree of freedom independently from others. In the second category of models, a capacity model defines a limit surface. When the load-deformation response of the element contacts the surface, the element's underlying model changes its hysteresis behavior to initiate strength loss and degradation. Examples of such models are presented in [6, 7]. While such models may define the onset of failure of one degree of freedom due to changes in another, they currently do not treat the full coupled behavior due to axial, shear and bending actions. Moreover, they are currently limited to only a subset of column failure modes.

A novel lumped-plasticity based computational element is proposed to address shortcomings listed above. The element uses behavioral models that define limit-state failure surface construct to trigger strength loss in

various degrees-of-freedom, while accounting for salient axial-shear-flexure interactions. The element and underlying behavioral models are intended to comprehensively treat all concrete column failure modes expected in building construction. The element is developed to explicitly simulate column nonlinear behavior up to complete loss of shear strength, moment strength and axial strength. The element aggregates a series of zero-length spring elements and an elastic line element that communicate with each other for coupling behaviors (Fig. 1). The elastic line element can adjust its stiffness based on the applied axial load. At the time of publication, the element was implemented in 2-dimensions as illustrated in Fig. 1, but will be expanded to full 3-dimensinal behavior including 3-dimentional flow rules in the near future. The element is offered in two formats. The first format is more traditional and requires the user to input all the behavioral model force-deformation relation parameters. This format is useful if absolute control over model behavior is desired. The second format is the automatic calibration format whereby the user only inputs column material and geometric properties, leaving the element and associated behavioral models to automatically define the backbone, cyclic and damage parameters. The behavioral models were calibrated to a large dataset of column tests. The ACI 369 column test database [22, 23] was used as the starting point with over 100 additional tests added to the set from the literature for a total dataset of over 600 column tests.

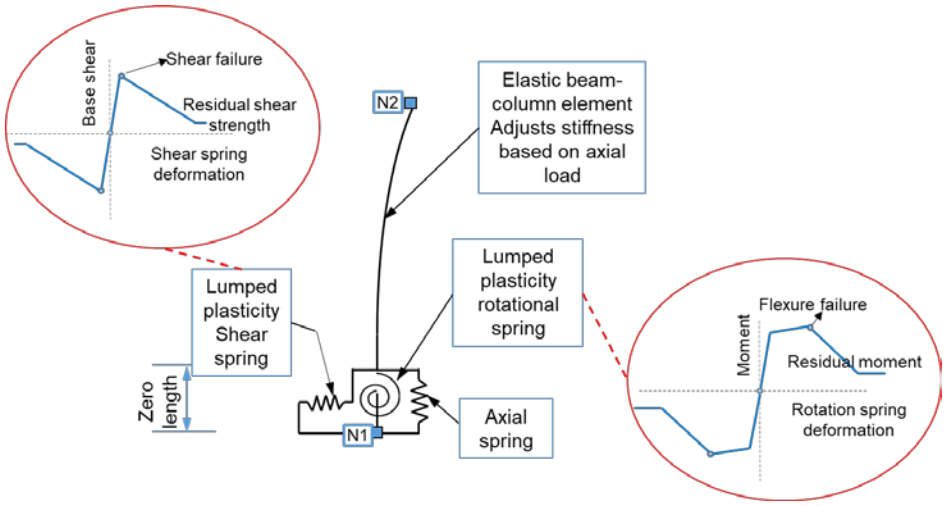

Fig. 1 Proposed computational element for considering axial/flexure/shear coupling behavior (2D version)

2.1 Rotation and Shear Behavior Models

2.1.1 Cyclic Behavior without Damage

The rotation and shear behavioral models are constructed using a typical force-deformation backbone either directly by the user or automatically through self-calibration (Fig. 2a). These model backbones can be defined non-symmetrically. Fourteen parameters are needed in total to define the backbone curve (seven parameters for each quarter). These parameters, shown in Fig. 2a for the moment-rotation behavior, are elastic stiffness (K_e), yielding moment (M_y), capping moment (M_c), capping rotation (θ_c) stiffness of degrading branch (K_d), residual moment (M_r), and ultimate rotation (θ_u).

To better represent the stiffness changes during cyclic lateral loading, a new spline curve model was implemented (Fig. 2b, Fig. 3). The behavioral models for rotation and shear only use three physically meaningful parameters to capture the key characteristics of column cyclic responses such as pinching effects. These parameters are the unloading stiffness, reloading stiffness, and energy ratio (Fig. 3). The energy ratio represents the energy inside the spline curve (gray dashed-line hatched area) divided by the maximum energy that could be dissipated denoted as the secant energy (green solid-line hatched area) as illustrated in Fig. 3b. The energy ratio accounts for the energy dissipated during cyclic loading and controls the pinching behavior. Applying a lower value of energy ratio leads to a more pinched behavior in this model as illustrated in Fig. 4.

Before reaching the capping strength, the cubic spline model uses peak-oriented rules to target the backbone curve such that the reloading path always targets the previous maximum displacement reached in that particular quadrant. In other words, target points may be different in each quadrant based on loading history. However, after exceeding the capping deformation in any direction of loading, the target point is now the peak prior deformation magnitude that was reached in any quadrant (Fig. 2b, steps 6 to 7 to 8). This latter rule was implemented to account for damage caused by excursions in one loading direction past the capping point on the behavior in the other loading direction. If the model is defined non-symmetrically, the target past capping is scaled based on the relative force and deformation values of the capping and residual points in each quadrant.

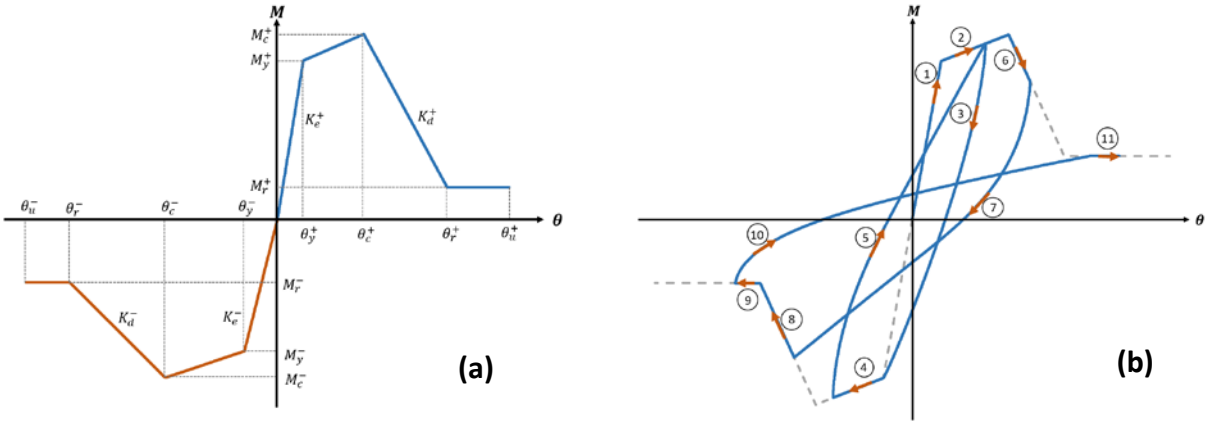

Fig. 2 a) Input parameters that define the backbone behavior for moment-rotation behavior. b) Hysteresis behavior of spline model without considering the damage model

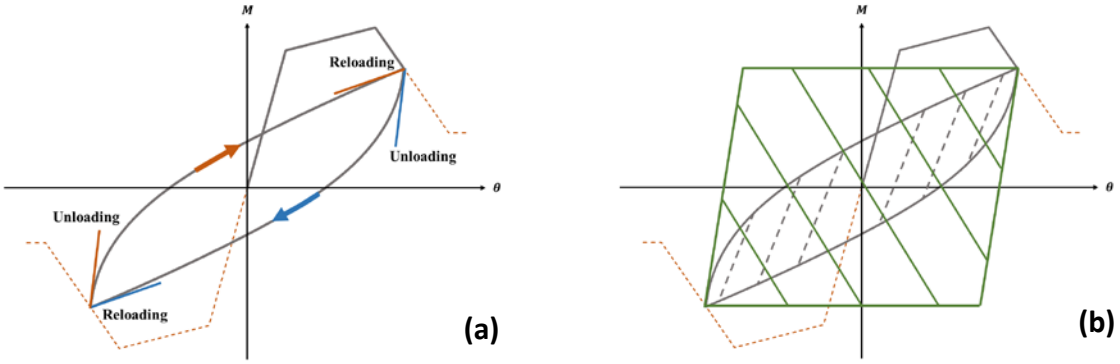

Fig. 3 Parameters needed to define spline curve including a) unloading and reloading stiffnesses, and b) energy ratio

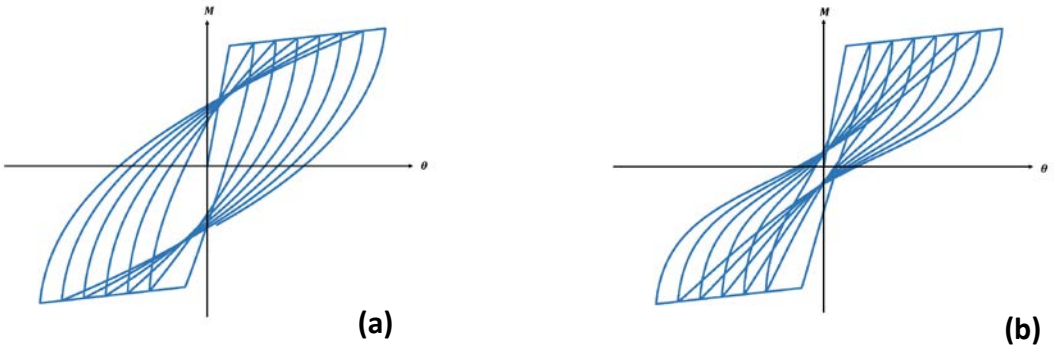

Fig. 4 Effect of energy ratio on pinching behavior; a) energy ratio of 0.6 and b) energy ratio of 0.2

2.1.2 Cyclic Damage Implementation

The rotation and shear behavioral models incorporate a damage model that can be triggered prior and/or after the capping point is exceeded. Different parameters can be defined for the two phases of behavior: 1) post yield but before capping, and 2) after capping. The damage model offsets the degrading branch of the backbone towards the force-deformation origin while the negative stiffness remains constant (Fig. 5a,c). The effect of the damage model prior to capping is to shift the capping point and ensuing degrading branch closer to the origin (Fig. 5a). No visible change in response therefore occurs due to the damage model being applied in the post-yield branch until the response reaches the adjusted capping point (Fig 5a). Once the response exceeds the capping point, the damage-model parameters for that phase are applied and the degrading branch continues to shift towards the origin (Fig. 5c). Damage cannot reduce the target load below the residual strength and therefore maintains the residual strength as a lower-bound strength.

The damage model calculates the energy under curve for every half cycle (Fig. 5b) and normalizes it by the area within the original force-deformation backbone. When load reversal takes place, based on the normalized energy, the descending branch in the opposite quadrant is shifted towards the origin, e.g. load paths number 3 and 4 in Fig. 5c. The proposed model is able to update the damage at every half cycle even without contact to the backbone. This feature makes the model capable to replicate realistic behaviors of structural responses under long duration ground motions where a large number of inner cycles are imparted that do not reach the backbone. Due to this functionality, the ability to accurately capture damage incurred in partial cycles that occur in different regions of behavior becomes important. The area under the curve for a given load path is subdivided into three separate regions and the area under the curve for each region is multiplied by a specific coefficient. Within the first region (green dotted in Fig. 5b), essentially elastic unloading can be expected and therefore limited damage to materials is expected. Consequently the coefficient C_1 multiplying the area for that region is likely to have a relatively low value. On the other hand, deformations incurred along the degrading branch of the backbone where never-before experienced deformations are sustained (orange dashed region in Fig. 5b) are expected to cause the most damage to the member, and so the C_3 coefficient is likely to have a relatively large value. The damage incurred per unit of energy dissipated within the intermediate range (gray shaded area in Fig. 5b) is expected to result in intermediate damage and therefore coefficient C_2 may be an intermediate value between C_1 and C_3.

3. Calibration of Model for Non-Retrofitted Concrete Columns

A comprehensive treatment of all behavioral models implemented in the proposed computational element is not possible within this paper. This section focuses on key novel aspects of the flexure and shear behaviors to highlight the capabilities of the computational model and illustrate sample coupling effects between behaviors.

3.1 Elastic Range of Behavior

In the linear elastic range of behavior, the most salient behaviors that the flexure and shear models capture include the effects of axial load on the stiffness, as well as moment and shear strengths of a column element. Prior studies [24] and national U.S. standards (e.g. [1, 2, 4]) have recognized the large shifts in column lateral stiffness due to variation in axial load. The elastic line element and rotational spring model in the proposed computational element monitor axial load on the element and adjust their elastic stiffness accordingly during analysis. Moreover, the rotational spring behavioral model adjusts the yield moment strength based on axial load during analysis and calculates it using the ACI 318-19 [4] stress block approach. The shear spring behavioral model also monitors axial load and adjusts the shear strength accordingly during analysis.

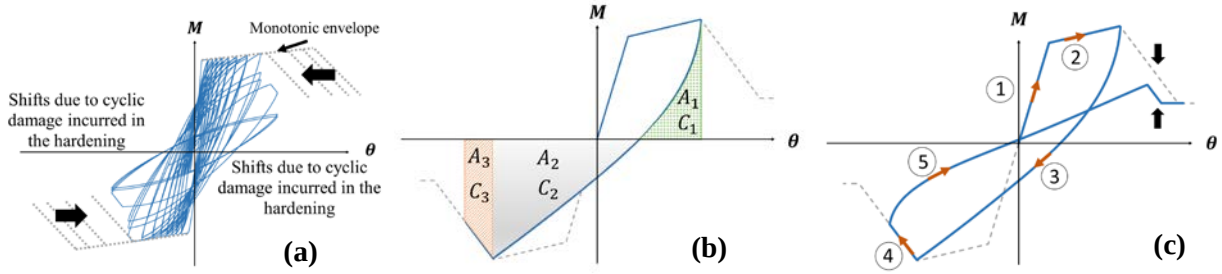

Fig. 5 Damage model: a) damage application in the pre-capping range, b) energy calculation, and c) applying damage based on normalized energy in the post-capping range

3.2 Post-Yield Range of Behavior

3.2.1 Backbone Parameters

After yield, the moment behavioral model calculates the capping or ultimate moment strength using 1.15 the steel yield strength and the ACI 318-19 [4] stress block approach. This moment strength is also adjusted continuously during analysis based on axial load. For shear, no hardening is expected if shear failure occurs and therefore the shear strength is maintained post-yield until the capping point.

Relations for the capping deformation at which strength loss initiates (Fig. 2a) were extracted from test data and implemented in the flexure and shear spring behavioral models. For example, for columns sustaining flexural modes of strength degradation such as loss of confinement and longitudinal bar buckling, the deformation at which moment strength loss initiates was found to be related to the normalized compressive axial load to cross-section area and concrete compressive strength ($N_u/A_g f_{cE}$), the spacing of the transverse steel normalized by the least column cross-sectional dimension (s/h_{min}), and the volumetric transverse reinforcement ratio adjusted by the ratio of transverse steel yield strength to concrete strength ($\rho_{t,vol}.f_{ytE}/f_{cE}$) (Fig. 6).

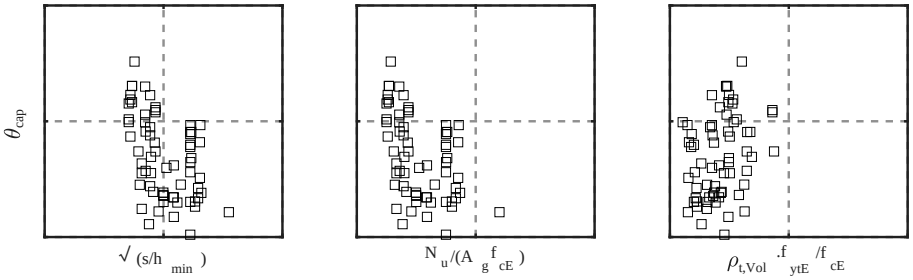

Fig. 6 Trends between the plastic rotation at capping and influential parameters for columns sustaining a flexural mode of strength degradation

3.2.2 Cyclic Parameters

As mentioned previously, only three parameters define the full cyclic behavior of the flexure and shear models. Relations were uncovered between the unloading (K_{unload}) and reloading (K_{reload}) stiffnesses and the secant stiffness to the contact point between the spline and backbone curves; the stiffness to that point is dubbed the secant stiffness (K_{secant}) (Fig. 7a). This relation is clearer for the reloading stiffness than the unloading stiffness (Fig. 7b,c). The shear and flexural models were therefore implemented to relate the unloading and reloading stiffnesses to the secant slope. Consequently, the unloading and reloading stiffnesses will soften as deformation increases and strength decreases.

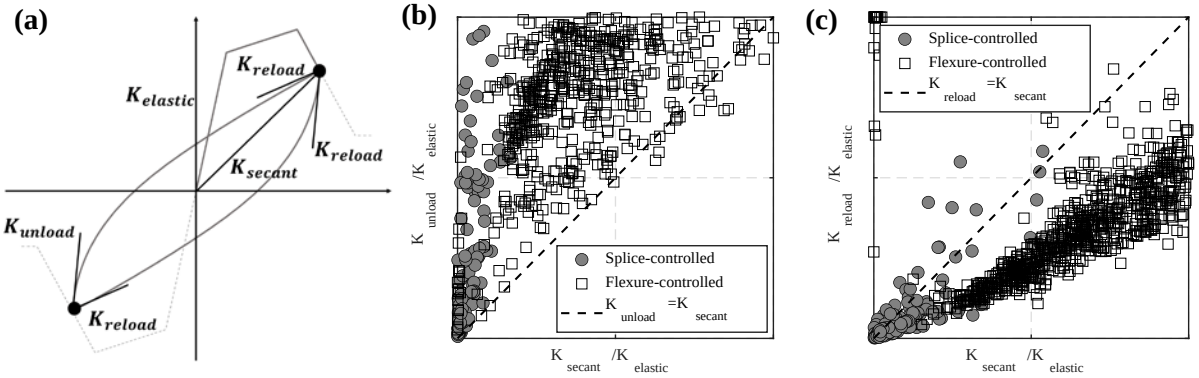

Fig. 7 a) Stiffness definition; b) trends between unloading (K_{unload}) and secant stiffness (K_{secant}); c) trends between unloading (K_{reload}) and secant stiffness (K_{secant}); data shown for columns sustaining a splice failure mode and flexural modes of failure.

Significant scatter was found when extracting the energy ratio from column experiments. The energy ratio in the post-yield behavioral range can be seen not to change with increasing deformation demands for columns deforming primarily in a flexural mode (Fig. 8a). Similarly, for columns in the post-yield behavioral range, the energy ratio does not appear to increase across the database of tests with increasing column deformation capacity to the capping point (Fig. 8b). This implies that a constant energy ratio can be defined for the post-yield behavioral range for flexure dominated behavior. Similar trends were observed for other deformation/failure modes of non-retrofitted columns.

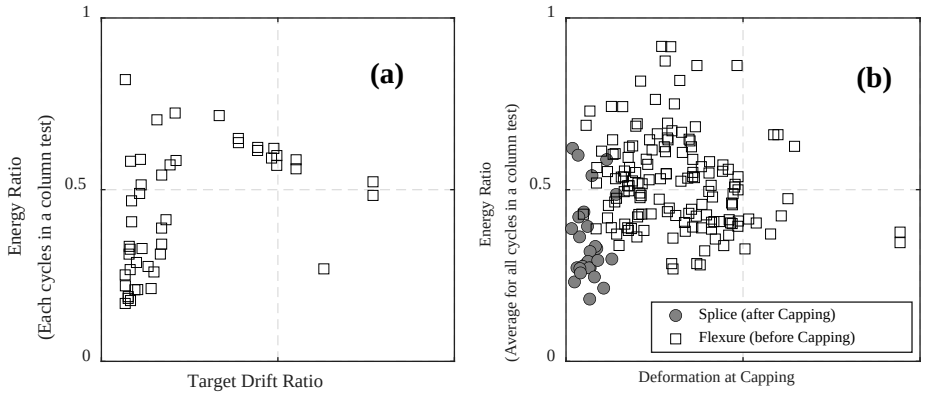

Fig. 8 Trends between the energy ratio and a) deformation demands for one column test and b) deformation capacities at capping for two groups of column tests

3.3 Post-Capping Behavior

The proposed element monitors all strengths and deformation capacities for each potential failure mode throughout the analysis. Once the first strength or deformation capacity is reached, either in the rotation

model or shear model, strength loss is initiated in that model while the other model unloads to maintain equilibrium as forces drop in the column element. In this strength degradation range, the model utilizes relations to define the degrading stiffness, residual strength, and cyclic parameters that can differ from those used in the post-yield pre-capping range. An ultimate deformation is also defined beyond which strength drop to essentially zero. Extraction of salient trends for test data was done in a similar fashion in this range of behavior as discussed for the previous range, and relations developed based on those trends such that the model can determine its parameters automatically in this range of behavior.

4. Calibration of Model for Retrofitted Concrete Columns

In a manner similar to non-retrofitted columns, data was extracted from tests of retrofitted columns using results of past studies. The data were classified according to column cross sectional shape (rectangular or circular), type of column deficiency (shear, lap-splice, or inadequate confinement), and jacketing material (steel or fiber-reinforced polymer). The laboratory specimens that make up the database were designed to reflect common deficient properties typically found in columns of older existing buildings. The proposed element in only applicable to columns that are adequately retrofitted to preclude the more brittle modes of failure and shift column behavior to become flexurally dominated. As such, nonlinear behavior of retrofitted columns is governed by the flexural model. This section presents the key aspects defining the performance of retrofitted columns.

4.1 Elastic Range of Behavior

In the linear elastic range, the stiffness of retrofitted columns is similar to that of non-retrofitted columns; it was found that steel and fiber jackets in columns do not increase the stiffness of concrete columns significantly.

4.2 Post-Yield Range of Behavior

Steel or fiber-reinforced polymer jackets increase concrete confinement and, consequently, concrete strength. Therefore, both the axial and flexural strengths of jacketed columns are increased due to retrofitting. Shear strength is also increased because of jacketing. Jackets have an effect on the construction of the backbone response, which is needed to define properties of the flexural behavioral model.

4.2.1 Backbone Parameters

Key parameters used to generate backbone curves consistent with ASCE/SEI 41-17 were extracted from the measured hysteretic response of jacketed columns. Key parameters needed for the computational model include the force at yield, the peak force, the drift at yield, the drift at 80% of peak force (capping point). Details of other parameters extracted from the jacketed column test database are presented by Alvarez and Brena (2018) [25]. The strength data extracted from test results were compared with simple models chosen to represent the yield and capping flexural strength of jacketed columns. As an approximation, yield flexural strength of jacketed columns was estimated using the ACI 318-19 stress block with a stress intensity equal to the confined concrete strength. The capping or ultimate moment strength was calculated using the ACI 318-19 stress block and a steel stress equal to 1.15 the steel yield stress to account for hardening.

4.2.2 Cyclic Parameters

Parameters for cyclic behavior rules of retrofitted columns were extracted from the database following an approach consistent with that from non-retrofitted columns. These parameters include the unloading and reloading stiffness ratios (Fig. 3a). Fig. 9 illustrates trends for secant stiffness (K_{secant}) with unloading (K_{unload}) and reloading (K_{reload}) stiffness, normalized to the extracted elastic stiffness ($K_{elastic}$) for FRP retrofitted rectangular columns. The trend indicates a relationship between unloading and reloading stiffness with the secant stiffness. This figure shows a high variability in the results, but unloading stiffness tends to be measurably smaller than the secant stiffness. Similarly, reloading stiffness tends to be smaller than the corresponding secant stiffness, but stiffer than the reloading stiffness.

Fig. 10 shows the relationship between the extracted capping deformation and energy ratio. The values of the energy ratios obtained at large capping deformations are, on average, smaller than those obtained at lower deformations (compare group 1 for columns with low capping deformation with group 2 for columns with larger capping deformation). This observation is consistent with higher pinching for the cycles of the columns with large capping deformations, which agrees with observations from past laboratory tests on retrofitted columns.

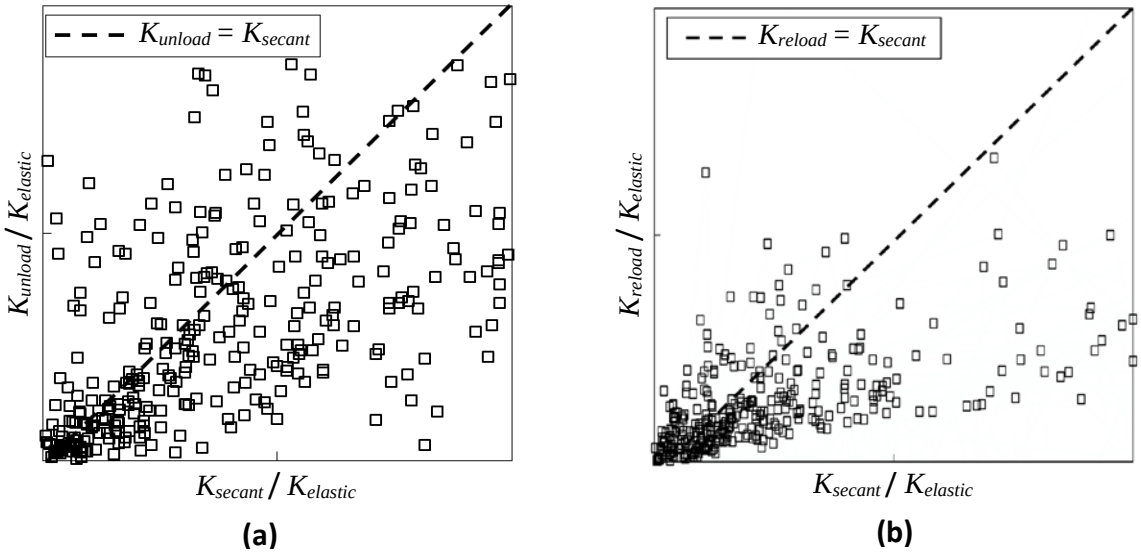

Fig. 9 Relations between unloading (K_{unload}) and reloading (K_{reload}) stiffnesses and the secant stiffness (K_{secant}) normalized by the elastic stiffness ($K_{elastic}$).

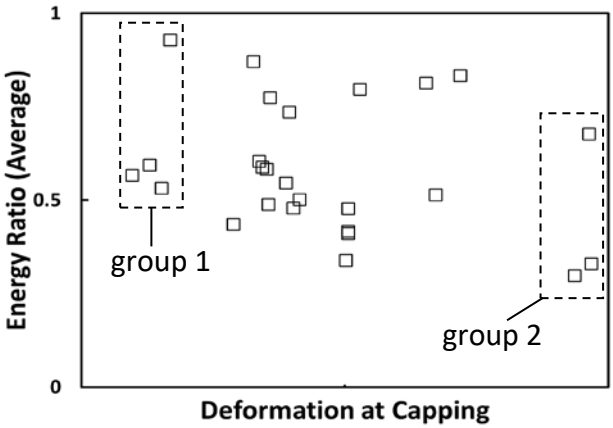

Fig. 10 Capping Deformation vs. Energy Ratio

4.3 Post-Capping Behavior

Most available test data of jacketed columns do not include enough information about post-capping behavior. At the time most of the jacketed column tests were conducted, it was typical to discontinue loading beyond a strength degradation of less than 80% of the capping strength. Therefore, the post capping behavior of retrofitted columns was assumed to be similar to that of non-retrofitted columns governed by flexural failure (not shear or lap-splice deficient columns). A calibrated model for non-retrofitted and FRP retrofitted rectangular columns (specimen C1 and C1FP1, tested by Harajli and Rteil 2004 [26]) is presented in Fig. 11. The model shows good agreement with test data.

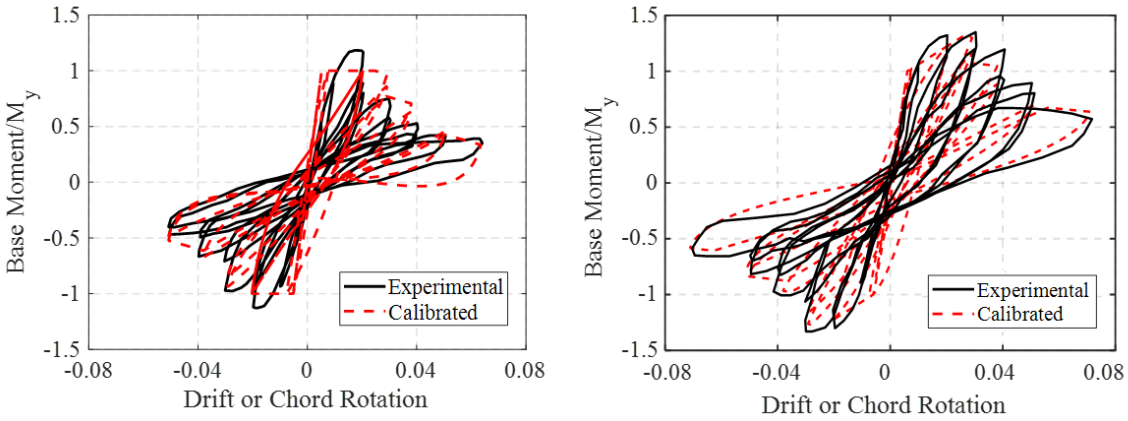

Fig. 11 Calibrated element vs. experimental data for retrofitted columns

5. Acknowledgements

The authors would like to acknowledge the National Institute of Standards and Technology for providing generous funding for the work presented through contract #70NANB17H241. The valuable insight and guidance of NIST researchers Siamak Sattar and Christopher Segura is gratefully acknowledged. The insightful input of Farzad Naeim and Ken Elwood is also gratefully recognized.

6. References

[1] ASCE/SEI (2017). Seismic rehabilitation of existing buildings (ASCE/SEI 41-17). Reston, VA, 623pp.

[2] ACI Committee 369 (2017). Standard requirements for seismic evaluation and retrofit of existing concrete buildings (ACI 369.1-17) and commentary, Farmington Hills, MI, 110 pp.

[3] Sattar S (2018): Evaluating the consistency between prescriptive and performance-based seismic design approaches for reinforced concrete moment frame buildings. *Engineering Structures* **174**: 919-931.

[4] ACI Committee 318 (2019). Building code requirements for structural concrete (ACI 318-19) and commentary. Farmington Hills, MI, 624pp.

[5] NEHRP Consultants Joint Venture (2013). Review of past performance and further development of modeling techniques for collapse assessment of existing reinforced concrete buildings (NIST GCR 14-917-28). Gaithersburg, MD, 210pp.

[6] Elwood KJ, Modelling failures in existing reinforced concrete columns. *Canadian Journal of Civil Engineering*, 2004. **31**(5): p. 846-859.

[7] Ghannoum WM, Moehle JP (2011): Rotation-based shear failure model for lightly confined RC columns. *Journal of Structural Engineering* **138**(10): p. 1267-1278.

[8] LeBorgne M, Ghannoum W (2013): Analytical element for simulating lateral-strength degradation in reinforced concrete columns and other frame members. *Journal of Structural Engineering*. **140**(7): p. 04014038.

[9] Panagiotakos TB, Fardis MN (2001): Deformations of reinforced concrete members at yielding and ultimate. *Structural Journal* **98**(2): p. 135-148.

[10] Juntanalikit P, Jirawattanasomkul T, Pimanmas A (2016): Experimental and numerical study of strengthening non-ductile RC columns with and without lap splice by Carbon Fiber Reinforced Polymer (CFRP) jacketing. *Engineering Structures*. **125**: p. 400-418.

[11] McKenna F, Fenves GL, Scott MH, Jeremie B (2000): Open system for earthquake engineering simulation, OpenSEES. https:// opensees.berkeley.edu/.

[12] ASCE/SEI (2016). Minimum design loads and associated criteria for buildings and other structures (ASCE 7-16). Reston, VA, 889pp.

[13] Spacone E, Filippou FC, Taucer FF (1996): Fibre beam – column model for non-linear analysis of R/C frames: Part I. Formulation. *Earthquake Engineering & Structural Dynamics*, **25**(7): p. 711-725.

[14] Limantono AA (2016): Modeling strain demands in longitudinal steel bars of concrete columns. Master Thesis, University of Texas, Austin, TX, 179pp.

[15] Clough RW (1966): Effect of stiffness degradation on earthquake ductility requirements. Report No. 66-16, Structural Engineering Laboratory, University of California, Berkeley, CA, 67pp.

[16] Bouc R (1967): Forced vibrations of mechanical systems with hysteresis. *Proc. of the Fourth Conference on Nonlinear Oscillations*, Prague: p. 315.

[17] Takeda T, Sozen MA, Nielsen NN (1970): Reinforced concrete response to simulated earthquakes. *Journal of the Structural Division*. **96**(12): p. 2557-2573.

[18] Baber TT, Wen YK (1981): Random vibration hysteretic, degrading systems. *Journal of the Engineering Mechanics Division*. **107**(6): p. 1069-1087.

[19] Baber TT, Noori MN (1985): Random vibration of degrading, pinching systems. *Journal of Engineering Mechanics*. **111**(8): p. 1010-1026.

[20] Ibarra LF, Medina RA, Krawinkler H (2005): Hysteretic models that incorporate strength and stiffness deterioration. *Earthquake engineering & structural dynamics*. **34**(12): p. 1489-1511.

[21] Lowes LN, Altoontash A (2003): Modeling reinforced-concrete beam-column joints subjected to cyclic loading. *Journal of Structural Engineering* **129**(12): p. 1686-1697.

[22] Ghannoum W, Sivaramakrishnan B, Pujol S, Catlin AC, Fernando S, Yoosuf N, Wang Y (2015): NEES: ACI 369 Rectangular Column Database, https://datacenterhub.org/resources/255.

[23] Ghannoum W, Sivaramakrishnan B, Pujol S, Catlin AC, Wang Y, Yoosuf N, Fenando S (2015): NEES: ACI 369 Circular Column Database, https://datacenterhub.org/resources/254.

[24] Elwood KJ, Eberhard MO (2009): Effective Stiffness of Reinforced Concrete Columns. *ACI Structural Journal* **106**(4): p. 476-484.

[25] Alvarez JC, Breña SF, Arwade SR (2018): Nonlinear Backbone Modeling of Concrete Columns Retrofitted with FRP or Steel Jackets. *ACI Structural Journal* **115**(1): p. 53-64.

[26] Harajli MH, Rteil AA (2004): Effect of Confinement Using Fiber-Reinforced Polymer or Fiber-Reinforced Concrete on Seismic Performance of Gravity Load-Designed Columns. *ACI Structural Journal* **101**(1): p. 47-56.

